ELSEVIER

Journal of Power Sources 67 (1997) 61–67

JOURNAL OF POWER SOURCES

# The tin effect in lead–calcium alloys

Nam Bui [a,*], Patrick Mattesco [a], Patrice Simon [a], Jean Steinmetz [b], Emmanuel Rocca [b]

[a] *Ecole Nationale Supérieure de Chimie de Toulouse, 31077 Toulouse, France*
[b] *Université Henri Poincaré Nancy I, 54506 Vandoeuvre-les-Nancy Cedex, France*

Received 8 August 1996; accepted 25 November 1996

**Abstract**

The effect of tin in the depassivation of lead–calcium alloys under conditions of deep discharge (0.7 V versus $Hg/Hg_2SO_4$ in 0.5 M $H_2SO_4$) is investigated by measurements of the polarization resistance, the oxidation rate of ferrous ions added to the electrolyte, the potential decay with/without applied cathodic current, and surface analysis and visual inspection. The results may help to choose the optimal level of tin in the alloys. © 1997 Elsevier Science S.A.

*Keywords:* Lead alloys; Tin; Depassivation; Calcium

## 1. Introduction

The use of low-antimony or antimony-free alloys is an effective means to minimize gassing and to achieve maintenance-free lead/acid batteries. Thus, new materials have been employed in grid manufacture, e.g. Pb–Ca alloys and even pure lead. Pb–Ca alloys have led to 'passivation' phenomena at the positive plate; these are attributed to the formation of a poorly-conducting oxide layer between the grid and the active mass [1]. This layer has been identified as tetragonal lead oxide, referred to as $\alpha$-PbO [2–4]. The formation of $\alpha$-PbO is induced by the presence of a lead sulfate layer that acts as a semi-permeable membrane and increases the local pH at the grid/lead sulfate interface to a value close to 9 [5,6]. Alloying with tin (the original objective of which was to improve fluidity during casting) was found to be effective in decreasing grid passivation. Tin decreases the thickness of the PbO layer [7,8] and increases the electronic conductivity of the passivation layer [9,10]. The mechanisms proposed in the literature range from a disproportionation reaction between PbO and SnO [11] to the formation of mixed, semi-conducting, Pb–Sn oxides [9,10]. In previous work [12,13], the authors have used electrochemical techniques to evaluate the electrical properties of the passivation layer. The results showed that the conductivity increases sharply for alloys with a tin content higher than 1.5 wt.%.

This study reports further investigations on the effect of tin. Several measurements have been carried out to elucidate the role of tin on the depassivation of Pb–Ca alloys under conditions of deep discharge.

## 2. Experimental

Pure lead and Pb–Ca–Sn alloys prepared by MetalEurop Recherche were used as working electrodes (Table 1). These alloys were heated to +600 °C, cast in a hot mould (300 °C), and then aged for 72 h at +60 °C. Working electrodes were imbedded in cold-mounting resin; their exposed surfaces were polished mechanically with emery paper under water (up to grade 1000), then washed in distilled water, and finally rinsed in absolute ethanol.

The electrochemical apparatus comprised a Radiometer IMT 101 Electrochemical Interface, DEA 332 Digital Electrochemical Analyser and ELDA 300 software with a Hewlett Packard Vectra 486 computer. Potentials were measured with respect to a $Hg/Hg_2SO_4$ reference electrode. The electrolyte was 0.5 or 4.5 M $H_2SO_4$. Polarization of the alloy electrode was in the potential range −1500 to 700 mV. The potential scan rate was 1 mV $s^{-1}$. Electronic conductivity of the passive layer, formed at 700 mV, was evaluated by following the current density related to the oxidation of $Fe^{2+}$ ions added to the sulfuric solution. The oxygen overvoltage was determined by direct measurement of the volume of evolved oxygen with the

* Corresponding author.


*PII* S0378-7753(97)02497-X

Table 1
Composition of test alloys studied [a]

| Name | Ca (ppm) | Sn (%) | Ag (ppm) | Al (ppm) |
|---|---|---|---|---|
| Pb–0.08Ca–0.6Sn | 795 | 0.60 | 34 | 143 |
| Pb–0.08Ca–0.6Sn–0.05Ag | 770 | 0.59 | 505 | 123 |
| Pb–0.08Ca–0.6Sn–0.1Ag | 759 | 0.58 | 1040 | 113 |
| Pb–0.08Ca–1.2Sn | 863 | 1.22 | 32 | 118 |
| Pb–0.08Ca–1.2Sn–0.05Ag | 775 | 1.22 | 495 | 94 |
| Pb–0.08Ca–1.5Sn | 800 | 1.50 | 32 | 140 |
| Pb–0.1Ca–2.0Sn | 960 | 2.10 | | 110 |
| Pb–0.1Ca–3.0Sn | 960 | 3.23 | | 120 |
| Pb–0.1Ca–5.0Sn | 920 | 5.50 | | 120 |

[a] Note, the number before each minor component (Ca or Sn) is the amount of that component in wt.% in the alloy.

eudiometric technique: oxygen gas was collected in an inverted burette filled with sulfuric solution.

## 3. Results

### 3.1. Potential decay measurements

The electrodes were maintained at 700 mV for 24 h in 0.5 M $H_2SO_4$, a condition that simulated deep-discharge; the polarization was then cut off. The change in the rest potential versus time for the alloys is shown in Fig. 1. For 0.6 wt.% Sn alloy, the potential dropped rapidly to the equilibrium potential of the PbO/Pb system and remained constant for a long time (more than 4 h). This feature indicates the development of a thick layer of PbO. With high-tin alloys (2 and 3 wt.% Sn), the self reduction of the oxides proceeded at high potentials for more than 4 h before attaining the PbO/Pb potential. This means that oxides with oxidation states higher than 2, namely $PbO_x$, were present in the oxide layer. At a very high tin level (5 wt.% in this case), there is a reverse effect, the amounts of PbO and $PbO_x$ are very small and the self-reduction takes place at low potentials before attaining the equilibrium potential of the $PbSO_4$/Pb couple. These results indicate

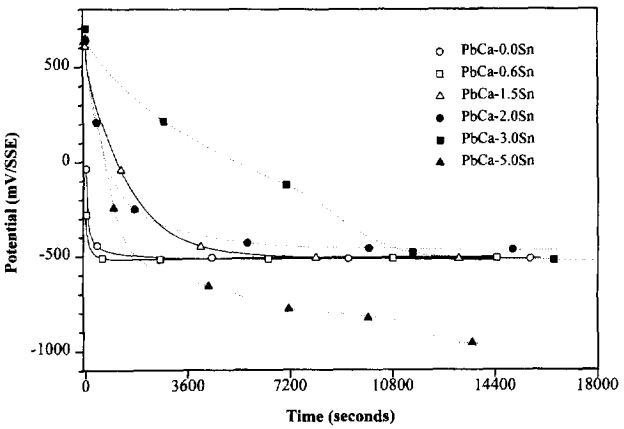


Fig. 1. Rest potential vs. time of Pb–0.08Ca–$x$Sn alloys after polarization at 700 mV for 24 h in 0.5 M $H_2SO_4$.

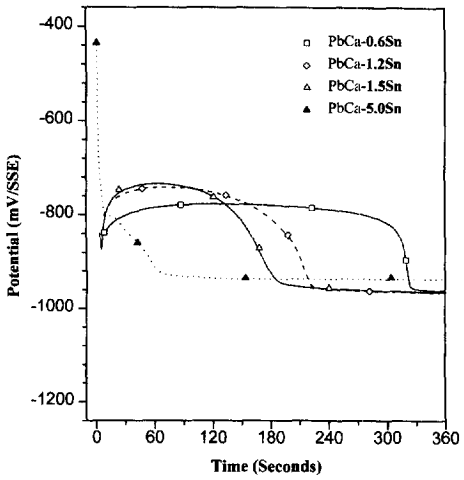


Fig. 2. Chronopotentiometry of lead alloys: effect of tin on the thickness of the PbO layer formed at 700 mV for 30 min in 0.5 M $H_2SO_4$. Reduction current = $-10^{-4}$ A cm$^{-2}$.

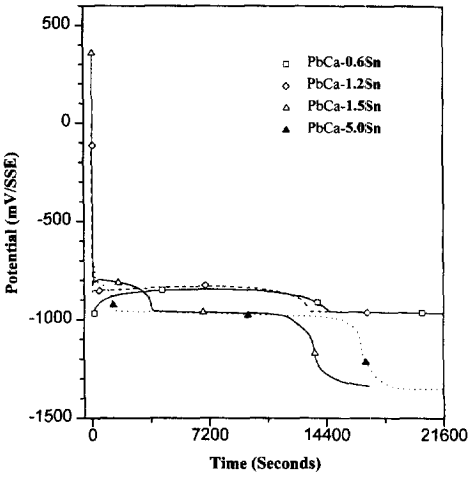


Fig. 3. Chronopotentiometry of lead alloys: effect of tin on the thickness of the PbO layer formed at 700 mV for 24 h in 0.5 M $H_2SO_4$. Reduction current = $-10^{-4}$ A cm$^{-2}$.

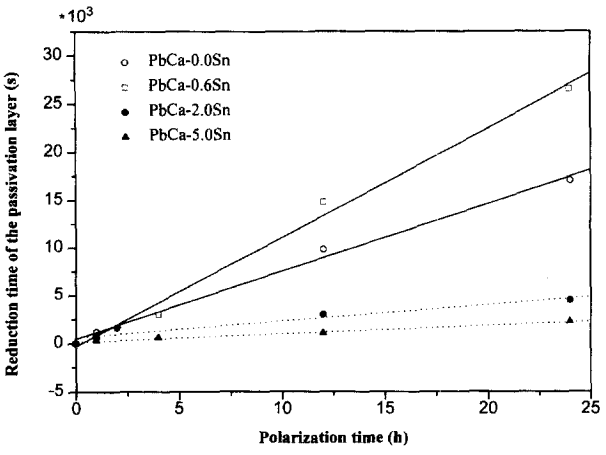


Fig. 4. Relationship between reduction time (proportional to the thickness of the passivation layer) and polarization time at 700 mV in 0.5 M $H_2SO_4$.

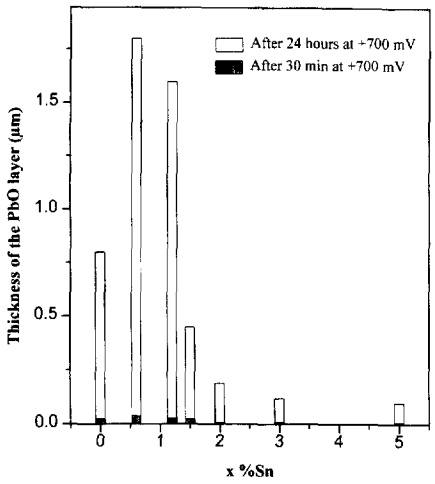


Fig. 5. Thickness of PbO layer on Pb–0.08Ca–$x$Sn after polarization at 700 mV for 30 min and 24 h.

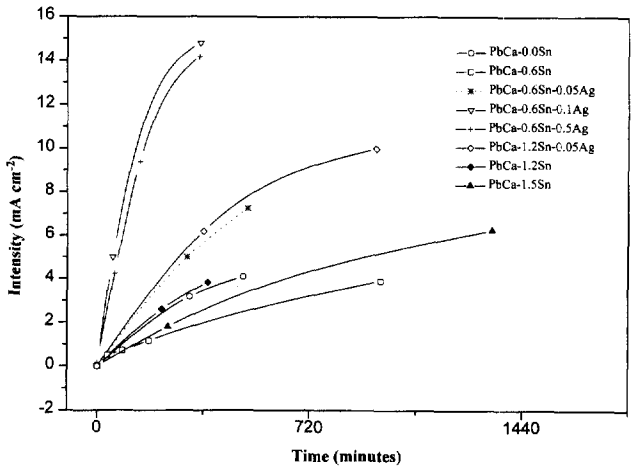


Fig. 6. Current density vs. time for different alloys during potentiostatic polarization at 1500 mV.

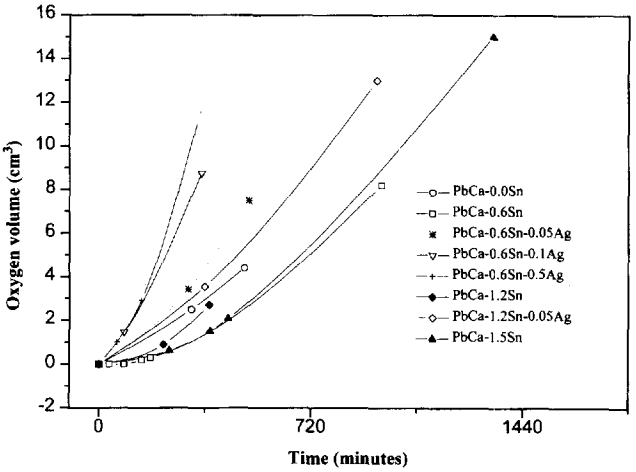


Fig. 7. Oxygen gassing volume vs. polarization time at 1500 mV for different alloys.

that tin favours the formation of $PbO_x$ at tin levels higher than 3.0 wt.%, but that the formation of PbO and $PbO_x$ is inhibited due to the presence of tin precipitates that produce a large amount of acidic tin ions during the anodic polarization, as shown later in this study.

### 3.2. Chronopotentiometry

The electrodes were polarized from −1500 to 700 mV at a scan rate of 1 mV $s^{-1}$ and were maintained at 700 mV for either 30 min (Fig. 2) or 24 h (Fig. 3). The reduction current was $-10^{-4}$ A $cm^{-2}$. It can be seen that the plateau potential that corresponded to $PbO_x$ (as described above) is not observable in Figs. 2 and 3. Thus, it can be assumed that the reduction current density was too high and the amount of $PbO_x$ too small to cause a potential arrest. In a previous paper [14], chronopotentiometry was performed with a reduction current of $-10^{-6}$ A $cm^{-2}$; the oxide formation time was 30 min at 700 mV. The potential plateau began at around −400 mV. In this study (i.e. with a reduction current of $-10^{-4}$ A $cm^{-2}$), the potential plateau was between −700 and −800 mV. The experimental plateau potential found by Ruetschi [5] for the PbO/Pb couple in 4.2 M $H_2SO_4$ was −380 mV. It seems that the intensity of the reduction current exerts an influence on the observed reduction potential: the higher the current, the lower the potential. Very low reduction currents may lead to the equilibrium potential of the redox system and, therefore, the plateau potential is approached. Nevertheless, the reduction must take place at a higher rate than the sulfation reaction, so the reduction current cannot be too low. The reduction time increased linearly with the oxidation time of the electrodes, see Fig. 4. The thickness of the PbO layer was calculated from the data of Figs. 2 and 3 and is plotted in Fig. 5. It is notable that the 0.6 wt.% Sn alloy exhibited the greatest thickness. The particular behaviour of this alloy can be observed in other reactions, for example, oxygen and hydrogen evolution. The thickness of the PbO layer decreased rapidly when the tin level was higher than 1.2 wt.%. The growth kinetics of the PbO layer appear to obey (over the studied period) a linear law versus the oxidation time — the thickness of the PbO layer determined by extrapolation of the data in Figs. 4 and 5 to seven days of oxidation was close to the value

Table 2
Comparison of the thicknesses of the PbO layer by linear extrapolation and by metallographic observation

| Wt.% Sn in alloys | 0.0 | 0.6 | 2.0 | 5.0 |
|---|---|---|---|---|
| Thickness of the PbO layer by linear extrapolation to 7 days (μm) | 5 | 8 | 2 | 0.7 |
| Observed thickness of the PbO layer after 7 days oxidation (μm) | 4.2 | 8.5 | 2.5 | 0.8 |

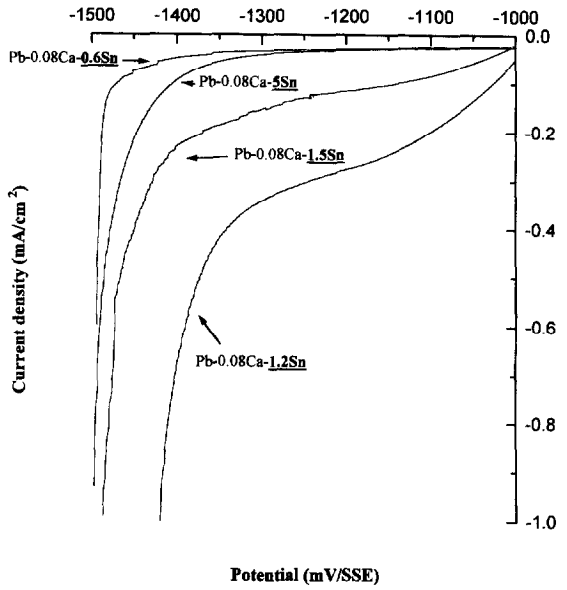


Fig. 8. Cathodic current for Pb–0.08Ca–$x$Sn electrodes relating to hydrogen evolution in 0.5 M $H_2SO_4$.

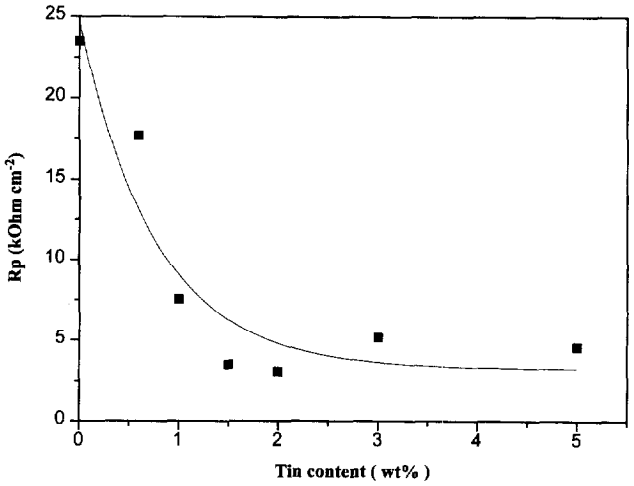


Fig. 9. Effect of tin on polarization resistance, $R_p$, of Pb–0.008Ca–$x$Sn alloys in 0.5 M $H_2SO_4$ after passivation at 700 mV for 24 h.

determined from metallographic observations of cross sections of electrode surfaces (Table 2).

### 3.3. Oxygen and hydrogen overvoltage

When the electrodes were polarized at 1300 mV, oxygen gassing was very limited. At higher potentials, the anodic currrent density and oxygen gassing both increased rapidly. At +1500 mV, anodic current densities of various alloys increased with time (see Fig. 6). As the electrodes are oxidized to give increasing amounts of $PbO_2$ [14], the anodic current is the sum of currents from the oxidation of the electrode and the oxidation of water. The latter reaction can be evaluated by eudiometric measurement of the volume of evolved oxygen. The effect of tin on the oxygen overvoltage is shown in Fig. 7. Note the behaviour of the 0.6 wt.% Sn alloy; it exhibits the highest overvoltage. In general, tin increases the oxygen overvoltage. On the other hand, alloying with silver lowers the oxygen overvoltage (Figs. 6 and 7). This silver effect has been reported previously by Pavlov and Rogachev [15].

To evaluate hydrogen evolution, the electrodes were polarized at −1500 mV, then the applied potential was increased and the cathodic current recorded. It was assumed that only the hydrogen evolution reaction occurred in the cathodic process, given the fact that lead hydride is formed only in small quantities [16]. Here again, the highest hydrogen overvoltage was displayed by the 0.6 wt.% Sn alloy and the general tendency is for alloying with tin to reduce hydrogen evolution (Fig. 8).

In general mechanisms proposed for the oxygen and hydrogen evolution reactions, it is proposed that O and H atoms are formed as intermediate products [17]. The rate-determining step is considered to be the combination of O or H atoms to form $O_2$ and $H_2$. Tin as additive may affect

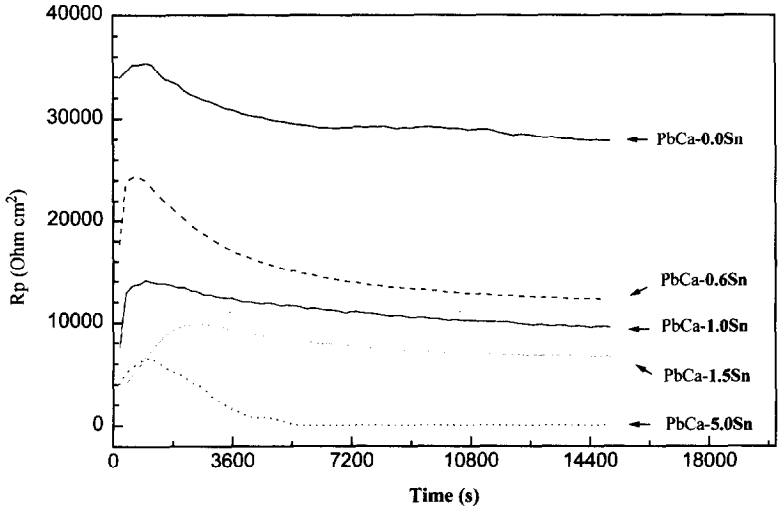


Fig. 10. Change in $R_p$ with time, at rest potential, after passivation at 700 mV for 24 h in 0.5 M $H_2SO_4$.

the combination reaction through the adsorption of atomic species. In the case of oxygen evolution, oxidized tin may change the phase composition of the anodic layer (to favour the formation of $PbO_x$) as well as the diffusion coefficient of the O species and, hence, the concentration of O atoms at the oxide-solution interface [15].

### 3.4. Conductivity of the passive layer

The effect of tin on both the resistivity and the electronic conductivity of the anodic layer was evaluated by measuring the polarization resistance ($R_p$) and the oxidation rate of ferrous ions dissolved in the sulfuric solution. The effect of tin on $R_p$, measured just after polarization of the electrodes at 700 mV for 24 h in 0.5 M $H_2SO_4$, is presented in Fig. 9. The polarization resistance dropped to a low level when the tin content was higher than 1.2 wt.%. This low level was roughly 5 k$\Omega$ cm$^{-2}$ for 3 and 5 wt.% Sn alloys. To assess the change in the anodic layer after polarization cut-out, $R_p$ was measured at two-minute intervals (Fig. 10). The increase in $R_p$ during the first hour indicates the discharge of $PbO_x$ to a less-conducting PbO. The subsequent decrease of $R_p$ may be related to a gradual transformation of PbO into $PbSO_4$ that is porous and less resistive. The rapid decrease of $R_p$ for the 5 wt.% Sn alloy is due to the small thickness of the PbO layer (Fig. 5).

The influence of layer thickness and time on the in situ conductivity of the PbO layer was assessed by measuring the oxidation rate of ferrous ions. The electrodes were passivated by potentiodynamic polarization from −1500 to 700 mV with a scan rate of 1 mV s$^{-1}$, then maintained at this potential for 3 min (thin anodic layer) or 24 h (thick anodic layer). Afterwards, ferrous ions, at a concentration of 0.025 M, were added to the 4.5 M $H_2SO_4$ solution. The oxidation current density of $Fe^{2+}$ was controlled by the

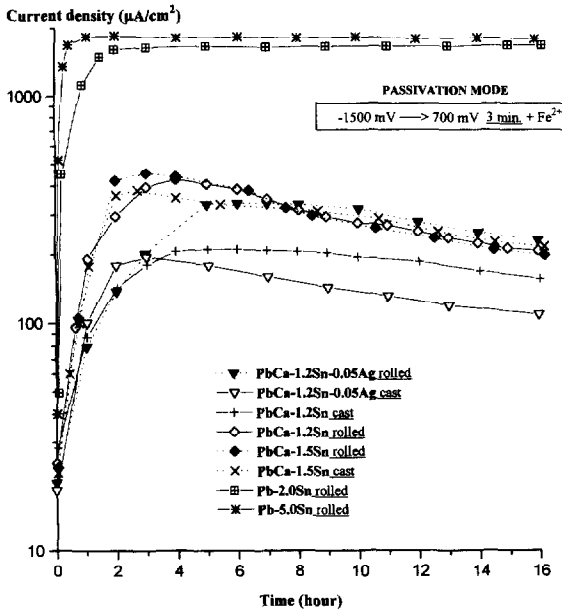


Fig. 11. Oxidation current density of $Fe^{2+}$ in 4.5 M $H_2SO_4$ vs. time at 700 mV on electrodes previously passivated for 3 min.

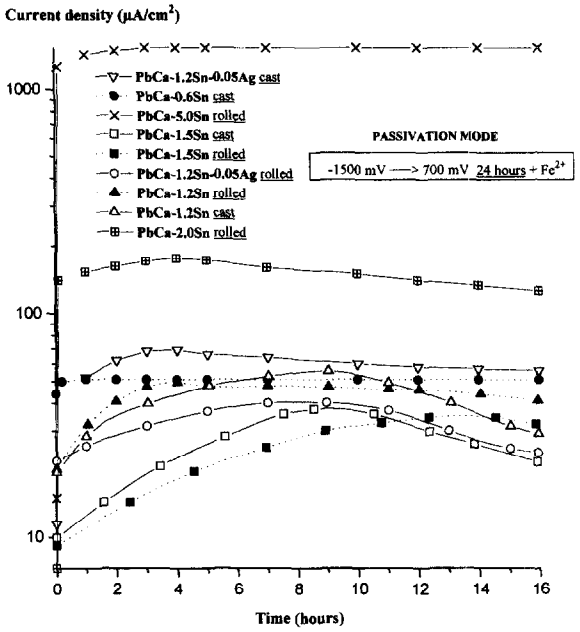


Fig. 12. Oxidation current density of $Fe^{2+}$ in 4.5 M $H_2SO_4$ vs. time at 700 mV on electrodes previously passivated for 24 h.

rate of transfer of electrons through the passivation layer. When there is no increase in the anodic current, it can be stated that there is no electronic conductivity to allow the oxidation of $Fe^{2+}$. For alloys containing only 0.6 wt.% Sn, no conductivity was observed after passivation for 3 min at 700 mV and only a very slight conductivity (increase of only 6 μA cm$^{-2}$) after passivation for 24 h. For alloys containing 1.2 or 1.5 wt.% Sn, the increase in oxidation current was considerable (i.e. few hundred μA cm$^{-2}$) when the passivation layer was thin (Fig. 11) and a few tens of μA cm$^{-2}$ when the passivation layer was thick (Fig. 12). This implies that the conductivity is closely related to the thickness of the PbO layer. It is worth mentioning that the oxidation currents reached a peak a few hours after the introduction of $Fe^{2+}$ ions to the sulfuric solution. The initial increase in conductivity can be explained by the increasing amount of conducting tin

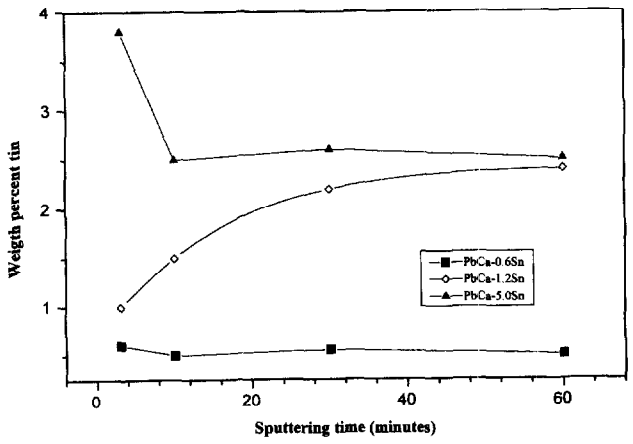


Fig. 13. Depth profile of tin in passive layers of Pb–Sn alloys formed at 700 mV for 24 h in 0.5 M $H_2SO_4$.

oxide in the PbO layer. The subsequent slight decrease of the conductivity can be explained by the increase of the thickness of the PbO layer and probably by the 'leaching out' of tin through dissolution in the sulfuric solution.

To verify if there is an enrichment of tin in the passivation layer, X-ray photoelectron spectroscopy (XPS) analyses were performed on electrodes polarized at 700 mV for 24 h in 0.5 M $H_2SO_4$ and with the resulting sulfate layers removed by treatment with 0.1 M acetate solution. The depth profile of tin in the passivation layer formed on Pb–Sn alloys is shown in Fig. 13. There is no enrichment of tin in the oxide layer for the 0.6 wt.% Sn alloy, a slight enrichment near the metal oxide interface for the 1.2 wt.% Sn alloy, and a decrease in the tin level for the 5.0 wt.% Sn alloy. These results are very different from the data obtained on Pb–Sn alloys passivated in pH 9 (tetraborate) solution [18] for which tin enrichment was considerable, since tin oxide has the lowest solubility in the pH 9 region [19]. In sulfuric solution, a dissolution of tin is expected and impedance spectroscopy studies [13] have shown an

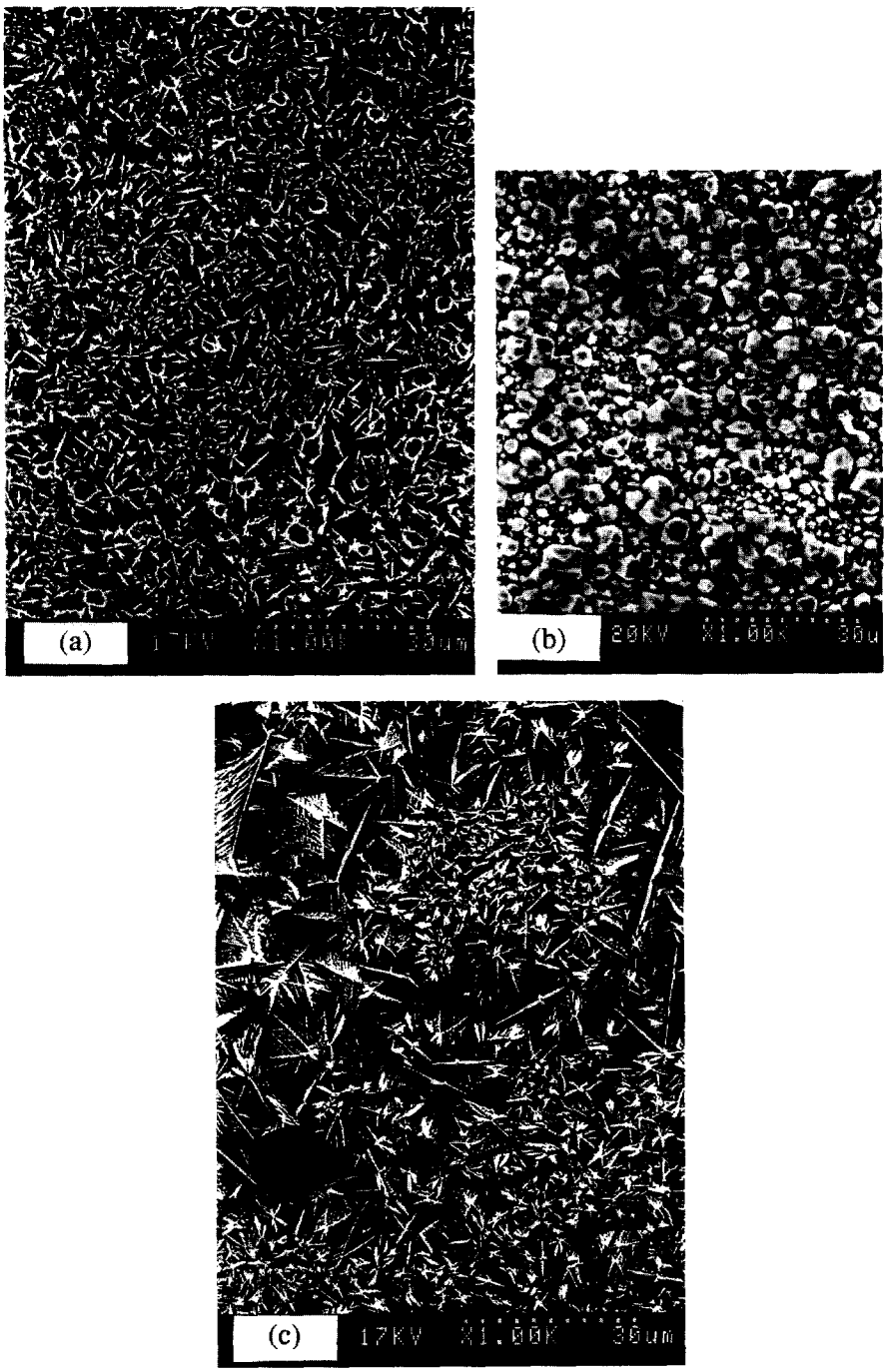


Fig. 14. Electron micrographs of electrode surface after polarization in 0.5 M $H_2SO_4$ at 700 mV: (a) for 2 min, alloy Pb–0.1Ca–5.0Sn; (b) for 24 h, alloy Pb–0.1Ca–5.0Sn, and (c) for 2 min, alloy Pb–0.008Ca–0.6Sn.

Table 3
Amount of dissolved lead and tin in 0.5 M $H_2SO_4$ after polarization at 700 mV for 7 days

| | Alloy | Pb–0.1Ca–0.6Sn | Pb–0.1Ca–2.0Sn | Pb–0.1Ca–5.0Sn |
|---|---|---|---|---|
| Pb | $\mu g\ ml^{-1}$ | 71 | 64 | 81 |
| Pb | $\mu mol\ cm^{-2}$ | 0.34 | 0.31 | 0.39 |
| Sn | $\mu g\ ml^{-1}$ | 0 | 28 | 88 |
| Sn | $\mu mol\ cm^{-2}$ | 0 | 0.24 | 0.75 |

increase in the ionic conductivity of the passivation layer due to the presence of tin ions.

Other experimental evidence to support the enrichment of tin in the passivation layer was obtained by metallographic observations and chemical analyses. When the tin content was higher than 2.0 wt.%, three phases were observed in the Pb–Ca alloys: a solid solution containing 1.9 wt.% Sn, fine precipitates $(PbSn)_3Ca$, and crystals (mostly coarse) of pure tin. The crystals can be readily dissolved in sulfuric acid, as shown by the micrographs of Fig. 14 where the dark holes relate to the sites of previously observed tin crystals and were formed when the 5 wt.% Sn alloy was polarized at 700 mV for only 2 min. With longer polarization times, the growth of $PbSO_4$ crystals covered these holes. Tin appears to retard the growth of $PbSO_4$ crystals since larger dendritic $PbSO_4$ crystals were observed on the 0.6 wt.% Sn alloy which displayed no tin precipitates and no related holes. To ascertain that there was dissolution of alloying tin, chemical analyses were carried out (with atomic absorption spectroscopy) to determine the amount of lead and tin in 0.5 M $H_2SO_4$ after polarization at 700 mV for seven days. The results are reported in Table 3.

For the particular 0.6 wt.% Sn alloy, tin was not dissolved in the sulfuric solution. For tin-rich alloys, however, the dissolution rate increased rapidly and in the case of the 5.0 wt.% Sn alloy, the molar dissolution of tin was almost twice that of lead.

## 4. Conclusions

The following conclusions can be drawn from the above studies.

1. Alloying with tin favours the formation of $PbO_x$ $(1 < x < 1.5)$ but high tin levels (> 3 wt.%) retard the growth of $PbO_x$ and PbO in the passivation potential range.

2. Over a period of seven days, a linear relationship is observed between the thickness of the PbO layer and the oxidation time at 700 mV.

3. Pb–0.008Ca–0.6Sn alloy exhibits a particular behaviour, namely, the greatest thickness of passivation layer and the highest oxygen and hydrogen overpotential.

4. Alloying with tin increases the overvoltage of the oxygen and hydrogen evolution reactions.

5. Under deep-discharge conditions, the alloyed tin level must be higher than 1.2 wt.% in order to increase the conductivity of the passivation layer.

6. The conductivity of the passivation layer increases with time; it then decreases when the thickness of the PbO layer increases and when tin is dissolved in the sulfuric solution.

7. The tin level must be higher than 1.5 wt.% to reduce the thickness of the PbO layer.

8. Alloying with tin reduces the growth rate of $PbSO_4$ crystals.

## Acknowledgements

The authors are indebted to the European Economic Community and to the European Advanced Lead-Acid Battery Consortium (Brite Euram Project BE 7297) for financial support.

## References

[1] K.R. Bullock and M.A. Butler, *J. Electrochem. Soc., 133* (1986) 1085.
[2] J. Burbank, *J. Electrochem. Soc., 106* (1959) 359.
[3] D. Pavlov, C.N. Pouliev, E. Klaja and N. Iordanov, *J. Electrochem. Soc., 116* (1969) 316.
[4] D. Pavlov and N. Iordanov, *J. Electrochem. Soc., 117* (1970) 1103.
[5] P. Rüetschi, *J. Electrochem. Soc., 120* (1973) 331.
[6] D. Pavlov and R. Popova, *Electrochim. Acta, 15* (1970) 1843.
[7] H.K. Giess, in K.P. Bullock and D. Pavlov (eds.), *Advances in Lead–Acid Batteries*, Proc. Vol. 84-14, The Electrochemical Society, Pennington, NJ, USA, 1984, p. 241.
[8] R. Miraglio, L. Albert, A.El. Ghachcham, J. Steinmetz and J.P. Hilger, *J. Power Sources, 53* (1995) 53.
[9] D. Pavlov, B. Monahov, M. Maja and N. Penazzi, *J. Electrochem. Soc., 136* (1989) 27.
[10] H. Döring, J. Garche, H. Dietz and K. Wiesener, *J. Power Sources, 30* (1990) 41.
[11] M. Terada, S. Saito, T. Hayakawa and A. Komaki, *Prog. Battery Solar Cells, 8* (1989) 214.
[12] P. Simon, N. Bui and F. Dabosi, *J. Power Sources, 50* (1994) 31.
[13] P. Simon, N. Bui, N. Pebere and F. Dabosi, *J. Power Sources, 55* (1995) 63.
[14] P. Mattesco, N. Bui, P. Simon and L. Albert, *J. Electrochem. Soc.*, submitted for publication.
[15] D. Pavlov and T. Rogachev, *Electrochim. Acta, 31* (1986) 241.
[16] A.F. Trotman-Dickinson, *Comprehensive Inorg. Chem., II* (1973) 115.
[17] M. Bockris and A.K.N. Reddy, *Mod. Electrochem., II* (1970) 1104.
[18] P. Simon, N. Bui, F. Dabosi, G. Chatainier and M. Provincial, *J. Power Sources, 52* (1994) 141.
[19] M. Pourbaix, *Atlas of Electrochemical Equilibrium in Aqueous Solution*, Gauthier–Villars, Paris, 2nd edn., 1974, p. 482.